Distribution Agreement

In presenting this thesis as a partial fulfillment of the requirements for a degree from Emory University, I hereby grant to Emory University and its agents the non-exclusive license to archive, make accessible, and display my thesis in whole or in part in all forms of media, now or hereafter now, including display on the World Wide Web. I understand that I may select some access restrictions as part of the online submission of this thesis. I retain all ownership rights to the copyright of the thesis. I also retain the right to use in future works (such as articles or books) all or part of this thesis.

Sarah Marie Narehood September 9, 2020

Optimization of Electron Bifurcating Photocatalytic System

By

Sarah Marie Narehood

Dr. Brian Dyer

Adviser

Chemistry

Dr. Brian Dyer

Adviser

Dr. Antonio Braithwaite

Committee Member

Dr. Eri Saikawa

Committee Member

2020

Optimization of Electron Bifurcating Photocatalytic System

By

Sarah Marie Narehood

Dr. Brian Dyer

Adviser

An abstract of

a thesis submitted to the Faculty of Emory College of Arts and Sciences

of Emory University in partial fulfillment

of the requirements of the degree of

Bachelor of Science with Honors

Chemistry

2020

Abstract

Optimization of Electron Bifurcation Photocatalytic System

By Sarah Marie Narehood

Electron bifurcation is a poorly understood energy conservation mechanism. The bifurcating process couples an exergonic redox reaction with an endergonic one. There are organisms that naturally utilize this pathway for anaerobic metabolism. In order to better understand this thermodynamically improbable mechanism, we designed a photocatalytic system that studies one of these natural, bifurcating systems. The [FeFe] hydrogenase from the organism *Thermatoga maritima*, and its natural redox partners, were incorporated into a photocatalytic system in order to study light-driven electron transfer. A CdSe/CdS nanorod was developed to be employed as the light-harvesting photosensitizer that initiated the electron transfer pathway. The result from this study showed successful development and characterization of the photocatalytic system. Electron transfer was able to be observed from the nanoparticles to the enzyme with clear results of electron bifurcation occuring.

Optimization of Electron Bifurcation Photocatalytic System

By

Sarah Marie Narehood

Dr. Brian Dyer

Adviser

A thesis submitted to the Faculty of Emory College of Arts and Science

of Emory University in partial fulfillment

of the requirements of the degree of

Bachelor of Science with Honors

Chemistry

2020

Acknowledgements

I am so appreciative for the support I received throughout my time at Emory, especially while conducting the research for this project and writing my thesis.

I am first, and foremost, grateful to Dr. Dyer. Thank you for welcoming me into your lab and giving me the opportunity to conduct such impactful research. I have learned so much through your guidance and mentorship, and I am forever indebted to the knowledge and experiences you provided me.

The next person, I would like to thank is Monica Sanchez. I do not even know where to start. Looking back now, I know that you truly shaped not only the researcher that I am today, but the person I am as well. I am so grateful to have had you as my mentor and as a friend.

I would also like to thank my lab. I was fortunate to have every one of you to help introduce me to the laboratory and research as a whole. As clueless as I was (and still am at times), you all were always patient and helpful. I am glad that I had you to receive guidance from in the lab, during project meetings, at conferences, and even about my future.

Finally, I would like to thank my Honors Thesis Committee. I know this is a difficult time to be taking on this type of commitment, so I am thankful for your help in getting me across this last leg of my undergraduate career.

There are so many more people that have been with me every step of the way, and I cannot even express how profoundly privileged I am to have you in my life.

Table of Contents

List of Figures

Chapter 1: Introduction

Electron bifurcation is the coupling of an exergonic reaction to promote an endergonic reaction. If better understood, this energy conservation mechanism could potentially be a replicable mechanism that is harnessed and reproduced in an array of fields. The motivation behind our research stems from the discoveries that were made when studying other biological energy conservation mechanism, like substrate-level phosphorylation and electron transport-linked phosphorylation.[1,2]

This poorly understood electron transfer pathway seems thermodynamically improbable, and yet, there are enzymes that naturally promote this process. An [FeFe] hydrogenase from the organism Thermatoga maritima (TmaHydABC) is one of these bifurcating enzymes. *Tma*HydABC undergoes electron bifurcation through a two-electron transfer (ET) process with two different, redox partners, nicotinamide adenine dinucleotide (NADH) and ferredoxin (Fdx). ET from these two redox pathways results in the reduction of protons leading to the production of H_2. The reduction potential of H_2 is -420 mV. With a midpoint potential of -453 mV, Fdx donates an electron to the enzyme in a downhill ET process.[3] The energy provided from this spontaneous oxidation reaction is the driving force for ET from NADH (midpoint potential of –320 mV) in this coupled uphill reaction. The red arrows show the energy landscape of this ET pathway in **Figure 1**. The gray, dashed-arrows show the non-native, oxidation of H_2 pathway.

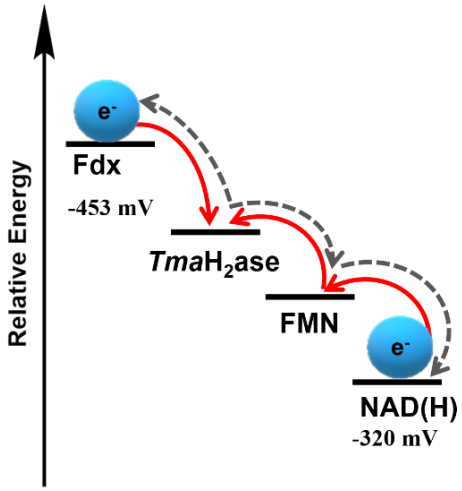

Figure 1: Illustration of the energy landscape for the proton oxidation (gray-dashed arrows) and reduction (red-bold arrows) TmaHydABC bifurcating pathway, which includes ferredoxin (Fdx), TmaHydABC [FeFe] hydrogenase ($TmaH_2ase$), flavin mononucleotide (FMN), and nicotinamide adenine dinucleotide, (NAD).

The mechanism of energy conservation accomplished by *Tma*HydABC is experimentally challenging to study as there are many factors involved in the process. However, developing a comprehensive model to describe the bifurcation mechanism is vital to understanding complex anerobic microbial metabolism.[4]

Our own research has been focused on studying this enzyme by incorporating it into a photocatalytic system. **Figure 2.A.** shows the photocatalytic system that was used. It was composed of our bifurcating *Tma*HydABC, its natural redox partners, Fdx and FMN, as well as a photosensitizer. By incorporating a light sensitive material, ET can be controlled, providing a clean and convenient way to promote bifurcation and study its mechanism. For the photocatalytic system in this study, CdSe based nanoparticles were used as the light sensitive material, as they offer high molar absorptivity and tunability of the band gap energy compared to alternative photosensitizers.[5] As indicated by the energy landscape of the photocatalytic system in **Figure 2.B.**, the light energy captured by the nanoparticles results in the excitation of electrons from the valence band of the semiconductor to the conduction band. The now excited electron undergoes

charge transfer from the nanoparticles to Fdx. The reduced Fdx can donate electrons to the *Tma*HydABC and initiate the first part of bifurcation.

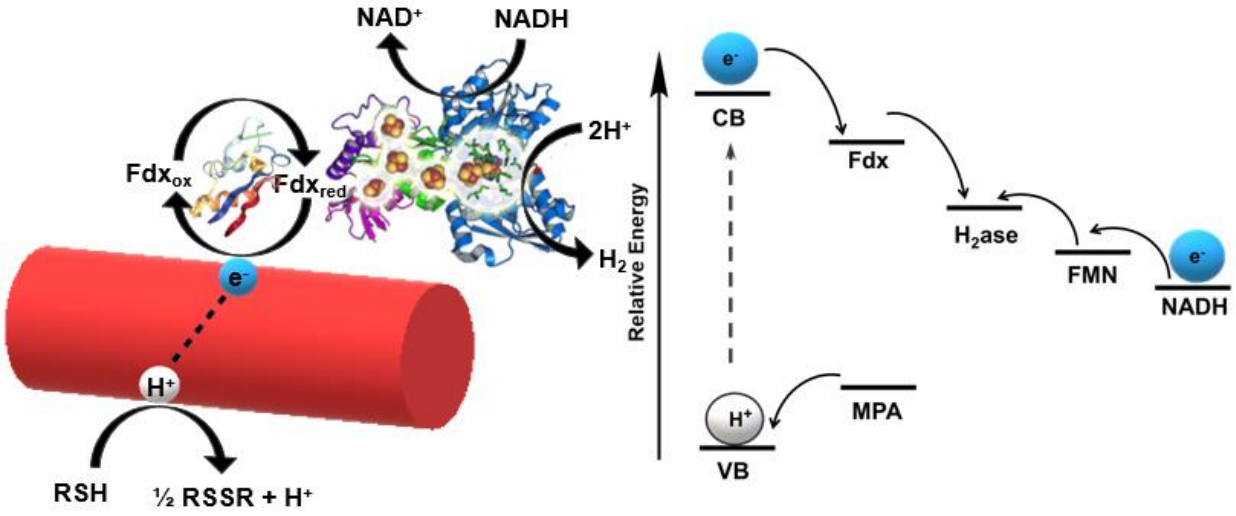

Figure 2: A. Depiction of ET pathway of the electron bifurcating photocatalytic system, with hydrogenase from *Clostridium pasteurianum.*[6] **B.** Energy landscape of photocatalytic system

A photocatalytic system requires preliminary characterization and optimization in order to understand the catalytic mechanism being studied. This includes developing optimal CdSe based nanoparticles that can be introduced into the system and successfully initiate electron transfer. After the optimization of the CdSe nanoparticles and their incorporation in the photocatalytic system, the ET pathway can be studied. We initially studied the interaction between the photosensitizer and the redox mediators, Fdx and FMN. With the results from these experiments, we were able to then study the entire ET pathway in the photocatalytic system through light-driven catalysis, the key experiment for studying electron bifurcation.

Chapter 2: Thesis Statement

We proposed that if *Tma*HydABC and its cofactors can be incorporated into a photocatalytic system, then we should be able to study electron bifurcation through light-driven ET transfer. In order to test this hypothesis, there were multiple experiments that needed to be conducted. These experiments were divided into three specific aims, which set out to create, characterize, and optimize the photocatalytic system. By completing each of these aims, we could establish a model bifurcating system and study the ET pathway of electron bifurcation.

2.1 Specific Aim 1

The photosensitizer was the first component of the photocatalytic system that needed to be studied. A CdSe based nanoparticle synthetic procedure was developed. The physical and electronic properties of these particles were then characterized. The particles, with the desired properties, such as uniformity in optical and morphological properties, were then incorporated into the bifurcating system.

2.2 Specific Aim 2

The interaction between the cofactors of the system and nanoparticles were then characterized to ensure efficient ET. Through light-induced ET, the interactions between the nanoparticles and the bifurcating *Tma*HydABC redox partners, FMN and Fdx, were studied.

2.3 Specific Aim 3

Finally, to establish optimal conditions for the bifurcating system, photo-driven hydrogen production assays were conducted. This experiment was also a clear method for determining if electron bifurcation was taking place.

Chapter 3: Methods and Approach

3.1 Synthesis of CdSeCdS Nanorods

3.1.1 CdSe Core Synthesis: Procedure was modified from a literature procedure.[7,8] Briefly CdO (0.08g), trioctlyphosphine oxide (TOPO), (4.8g), and hexyl phosphonic acid (HPA) (0.78g) were combined in a three-bottle-neck flask and put under vacuum, while heating to 150 °C for 2 hrs. After which, the reaction vessel was put under N_2 atmosphere. Once under N_2, the flask was heated to 250 °C until the reaction mixture went clear, indicating that the Cd had fully dissolved in the solvent. Once the reaction mixture became clear, the Se precursor solution was injected. At first appearance of a color change, the vessel was removed from heat and cooled to room temperature. A small addition of hexane was added to keep the reaction mixture in solution phase.

The Se precursor solution was prepared by dissolving 0.2 g of Selenium into 3.64 mL of trioctylphosphine (TOP).

3.1.2 CdS Shell Synthesis: A CdS shell was grown around the nanorod using a modified procedure from the literature.[9] Briefly CdO (.06g), TOPO, (3g), octadecyl phosphonic acid (ODPA)* (0.29g), and hexyl phosphonic acid (HPA) (.08g) were combined in a three-bottle-neck flask and put under vacuum, while heating to 150 °C and stirring for 2 hrs. After which, the reaction vessel was put under N_2 atmosphere. Once under N_2, the flask was heated to 300 - 350 °C until the reaction mixture went clear, indicating that the Cd has fully dissolved in the solvent. Once the reaction mixture was clear, 1.5 mL of TOP was injected. Once the desired reaction temperature recovered to ~340 °C the S precursor solution was injected. At first appearance of a color change, vessel was removed from heat and cooled to room temperature. A small addition of hexane or toluene was added to keep the reaction mixture in solution phase.

The S precursor solution was prepared by dissolving 0.12 g of Sulfur and 1-2mL of washed CdSe core particles into 2 mL of TOP. The sample was placed under nitrogen for 20 minutes before injecting into the Cd precursor.

*ODPA was purchased from Alfa Aesar

3.1.3 Ligand Exchange Procedure: Procedure was modified from a literature procedure.[8] The nonpolar ligand was exchanged with mercaptopropionic-acid (MPA) via ligand exchange procedure. Briefly, 5mg of purified nanorods was refluxed for 2hrs under N_2 in the dark in 15mL of MeOH with 76.1 mM MPA. The pH of this reaction mixture was adjusted to 10 using Tetramethylammonium hydroxide (TMAOH) prior to refluxing. After the reaction went to completion, the exchanged nanorods were then isolated by centrifugation and resuspension in 10 mM MPA, 10mM Tris(2-carboxyethyl)phosphine (TCEP), 50 mM Borate buffer and stored in an air free environment for future use.

3.2 Characterization of CdSeCdS NRs

3.2.1 Transmission Electron Microscopy (TEM): TEM images of the nanorods were taken in order to evaluate the structural properties. A sample of 2mg purified NR's were dissolved in organic solvent (hexane/chloroform) and pipetted on carbon side of copper TEM films.

3.2.2 UV-Vis Absorbance: An absorbance measurement of the nanorods was taken with a PerkinElmer Lambda 35 UV/Vis Spectrometer A quartz cuvette, with pathlength 1cm, was filled with chloroform and used as blank. After measuring 100% transmission, a couple drops of the nanoparticles were added to the cuvette until enough color was detectable without oversaturating the sample. The UV-Vis spectrum of the particles was then measured and saved for analysis.

3.2.3 Fluorescence: A fluorescence measurement of the nanorods was taken with a Horiba Duel-Fl. A quartz cuvette, with pathlength 1cm, was filled with chloroform and a couple drops of nanoparticles were added until enough color was detectable without oversaturating the sample. The cuvette was placed in the instrument and excited with 532nm light. The fluorescence measurement was then saved for analysis.

3.2.4 Quantum Efficiency (QE): The sample contained CdSe/CdS nanorods (0.1-0.2 O.D.) and 5 mM DQ03, a previously studied bipyridine mediator.[5] The total volume for each sample was 1.4 mL in 50 mM phosphate buffer, pH 7.1. The sample was prepared inside of a glovebox and buffer exchanged prior to use. The cuvette was sealed with an air-tight topper and removed from glovebox. During the experiment, N_2 flow as introduced 10 min prior to the start of the experiment and continuously run through the headspace of the cuvette to prevent O_2 contamination. The sample was also stirred continuously.

The sample was illuminated with a 405 nm* diode (from thor labs) and the absorbance monitored with a fiber optically coupled ocean optics Uv-visible spectrometer. The sample was illuminated in 10 second intervals and allowed to equilibrate for 10 seconds. This process ensured that the sample was not O_2 contaminated which would result in artificially lower QE.

*The same procedure was repeated with the 532nm diode.

3.3 Pymol of *Thermatoga martima* Ferredoxin

Pymol software program was used to characterize the charged surface of Fdx. This structure provided a visualization to where the nanoparticles, with a negatively charged capping ligand, would electrostatically interact with a positively charged region of Fdx.

3.4 Photoluminescence Quenching Experiment

A steady-state fluorescence quenching assay was performed to better understand the binding behavior of Fdx to the surface of the nanorods. In a 384-well, black microplate, increasing concentrations of Fdx were aliquoted into each well, which contained a uniform volume of nanorods or buffer. The plate was prepared in a glovebox, and the samples were buffer exchanged with 50mM sodium phosphate buffer, pH 7.99. Before removing the plate from the glovebox, a clear film was placed over the wells to keep the samples air free.

The fluorescence measurements were taken on a Biotek microplate reader. The plate was placed in the instrument and then each well was excited with 532nm light.

3.5 Steady-state Photoreduction

3.5.1 Photoreduction of Fdx: The sample consisted of 0.02 mM *Tma* Ferredoxin and (0.1-0.2 O.D.) CdSeCdS nanorods combined in a cuvette with a total volume 1.3mL in 50mM sodium phosphate buffer with 50mM MPA, pH 7.99. The sample was prepared and buffer exchanged in an oxygen-free glove bag. The cuvette was capped with air-tight topper and taken out of the glove box.

The sample was illuminated with a 532 nm diode (from thor labs). The initial absorbance spectrum and the change in absorbance was monitored with a fiber optically coupled ocean optics Uv-visible spectrometer.

3.5.2 Photoreduction of FMN: The previous procedure was repeated with 0.1mM FMN.

3.6 Hydrogen Production Assay

Similar to the photoreduction experiments, for typical hydrogen production assays the samples were combined in a cuvette, which consisted of 0.1 mM *Tma* Ferredoxin, (0.1-0.2 O.D.) CdSeCdS nanorods, 1mM NADH, 200 nM FMN, and 200nM *Tma*HydABC. The total volume

was 1.4 mL in 50mM sodium phosphate buffer with 50mM MPA, 7.5 pH. The sample was prepared and buffer exchanged in an oxygen-free glove bag. The cuvette was capped with air-tight topper and taken out of the glove box. The concentrations of FMN and Fdx were varied depending on the experiment. At times, the concentration of FMN was varied from 0.1 mM to 200 nM, but the optimized conditions were mentioned above.

The sample was illuminated with a 532 nm diode (from thor labs). The initial absorbance spectrum and the change in absorbance was monitored with a fiber optically coupled ocean optics Uv-visible spectrometer. The amount of H_2 generated was monitored with a pressure sensor. The pressure sensor was inserted into the cap of cuvette. The change in pressure recorded was used to determine the moles of H_2 generated with this method.

Chapter 4: Results and Discussion

4.1 CdSe/CdS Characterization

There are a wide variety of nanoparticles that are being utilized in many fields of research. One of the most prominent structures is the quantum dot (QD). CdSe/CdS dot-in-rod (DIR) nanoparticles offer light harvesting capabilities that can be utilized in photocatalytic systems. However, there are other light-sensitive components of the catalytic system that must be considered. For example, the bifurcating hydrogenase's redox partner, NADH, absorbs light at 260nm and 340nm, as shown in **Figure 3**. Even with the addition of a CdS shell, the quantum dot still absorbs in the near UV region of the absorbance spectrum. It was observed in the literature that the physical structure of the nanoparticle must be altered in order to change the electronic properties.[7]

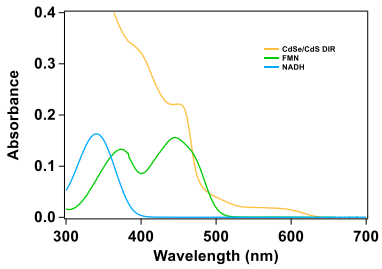

Figure 3: Absorbance spectra of CdSe/CdS dot-in-rod (DIR), flavin mononucleotide (FMN), and nicotinamide adenine dinucleotide (NADH)

In developing a synthetic procedure for a new CdSe/CdS nanorod structure, we created a photosensitizer that absorbed light in the intended region of the light spectrum, where there would be no other cofactor absorbance interfering. The inorganic bulk material, that was used,

poised the excited state electron at the right energy level for efficient ET. The initial procedure produced CdSe nanoparticles that were thicker and shorter in structure, as shown in **Figure 4.A**. The addition of n-hexylphosphonic acid (HPA), with ODPA, led to a more rod-like structure. The HPA ligand oriented the crystalline structure to grow in one direction leading to a longer, rod shape. **Figure 4.B.** shows an image from an initial synthetic procedure using HPA. The ratio of starting materials was adjusted until the nanoparticles were the desired, uniform shape, as shown in **Figure 4.C**. A final step of the synthetic procedure was the addition of a CdS shell around the CdSe nanorod. The shell provides a physical barrier that allows for a longer-lived exciton by hindering charge recombination. **Figure 4.D** shows the final, optimized CdSe/CdS rod-in-shell nanoparticles.

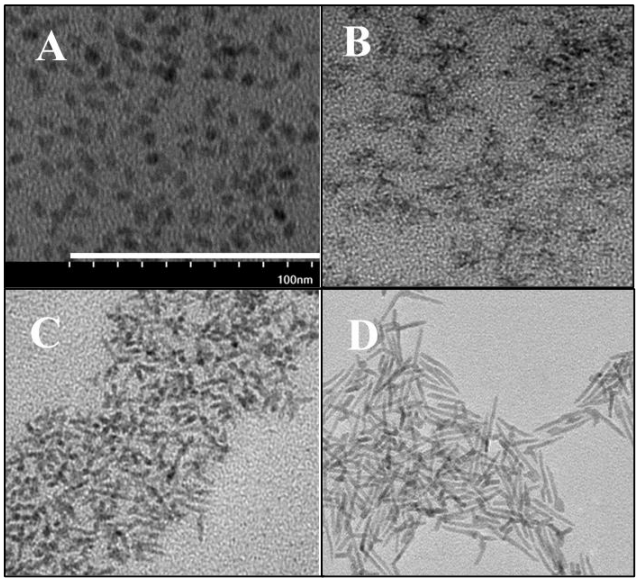

Figure 4: **A**. Initial CdSe nanoparticles **B.** CdSe nanoparticles grown in presence of HPA **C.** CdSe nanoparticles with adjusted solvent conditions **D.** CdSe/CdS rod-in-shell structure. The white bar in panel **A** can be used to judge the approximate length and width of particles in panels **B-D** as well.

As predicted, the UV-Vis absorbance spectrum of CdSe nanorods showed red-shifted. features as compared to the CdSe/CdS DIR nanoparticles when we elongated the core from a quantum dot to a rod structure. The addition of the CdS shell grown around the CdSe nanorod produced even more distinct absorbance features, which indicates more uniform particles. The spectra can be observed in **Figure 5.A**. The nanorods also emitted significant fluorescence when excited at 532nm light, as shown in **Figure 5.B**. The figure also shows how the addition of the CdS shell results in a much longer-lived exciton.

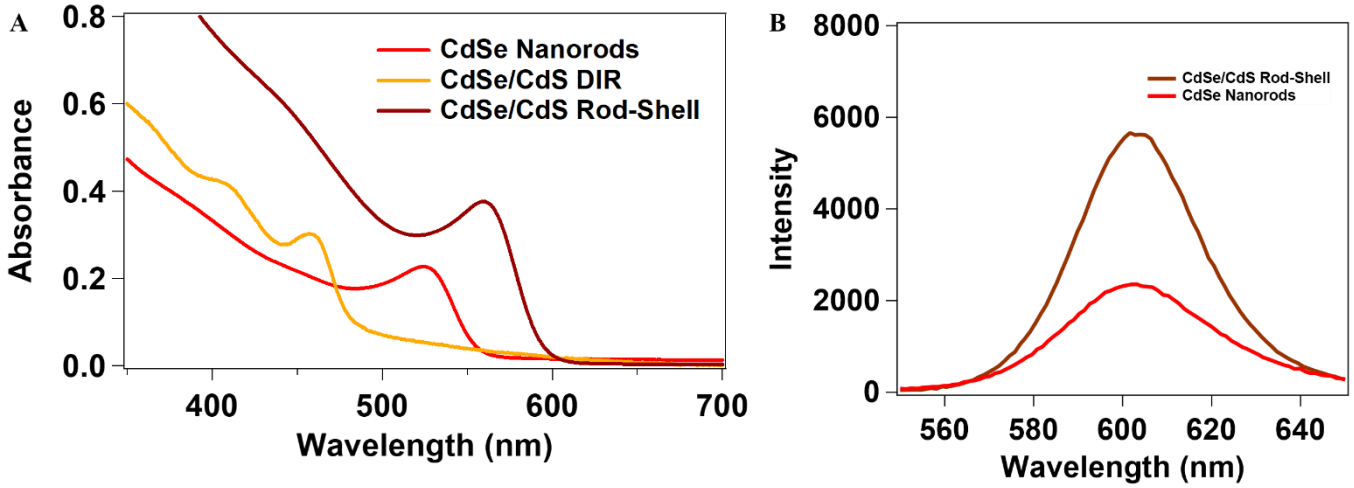

Figure 5: A. UV-Vis absorbance spectra of CdSe nanorods, CdSe/CdS DIR, and CdSe/CdS Rod-Shell **B.** Fluorescence emission of CdS/CdS Rod-Shell and CdS nanorods excited at 532 nm

A final characterization of the nanoparticles was measuring the QE. QE helped us understand the ET between the particles and a mediator. It made clear whether or not the particles can efficiently participate in ET. The moles of mediator radical generated was divided by the mols of photons absorbed, as shown in **Equation 1**. The index of refraction was accounted for by multiplying by 9.15, which was derived from previous measurements. [5]

$$QE = \frac{Mols\ of\ mediator\ radical}{Mols\ of\ photons} \qquad \textbf{Equation 1}$$

In order to calculate QE, we had to conduct a photoreduction assay where we probed the nanoparticles with light and monitored the ET transfer between these particles and a mediator.

For this experiment we used DQ03, which has been previously determined in the literature as an optimal redox mediator when working with CdSe based nanoparticles. **Figure 6.A.** shows the entire visible spectrum with the change in absorbance of reduced mediator being monitored over 200 seconds. We isolated a wavelength that was specific to the generated mediator radical (504nm) and monitored the change in absorbance at this wavelength over time. **Figure 6.B.** shows the QE of the nanoparticles when probed with 405 nm and 532 nm light. Even with 25% QE, it was determined that these particles could be used for enzymatic studies.

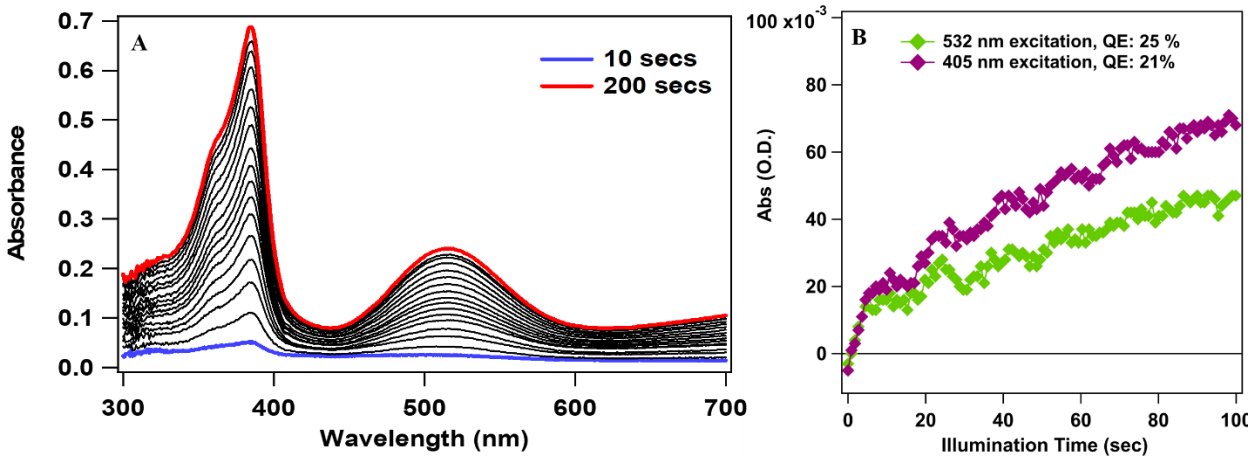

Figure 6: A. Change in absorbance of photo-reduced DQ03 over time. **B.** QE measurements for CdSe/CdS with excitation at 532nm and 405nm light.

4.2 Photosensitizer and Fdx Interaction

The initial electron transfer between Fdx and the nanoparticles is a crucial interaction to understand when considering the efficiency of the electron bifurcation mechanism. Analyzing the Pymol file of the charged surface area of Fdx, there were positively charged sites at the surface of the FeS cluster on the Fdx structure. **Figure 7.A.** shows the ribbon depiction of Fdx. The FeS clusters can be easily located. With the inclusion of the surface charged feature, there appeared a blue region, which was indicative of a positively charged region on the surface of the protein near the site of the FeS cluster. Presumably positively charged region, is the electron

storage site that is also a likely position for electrostatic interactions with the negatively charged surface of the nanoparticles. These structures can be seen in **Figure 7.A.** and **7.B**.

To better characterize the interaction between the nanoparticles and Fdx, a

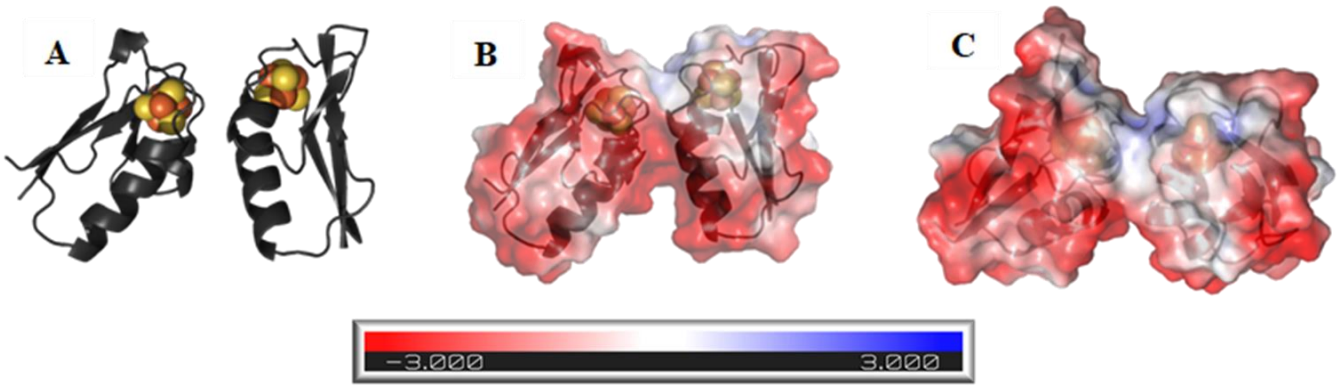

Figure 6: A. Ribbon structure of Ferredoxin from *Pyrococcus furious* (PBD: 2z8q) **B.** Overlapping ribbon and charge surface structure of Fdx **C.** Charged surface area of Fdx

photoluminescence quenching assay was conducted. Through this experiment, wecould determine the binding constant of Fdx to the surface of the particles . As the concentration of Fdx is increased the fluorescence of the nanoparticles decreased, indicating that Fdx quenched the excited state electron and ET occurred. **Figure 8.A.** shows the decreasing trend in fluorescence with the increase in Fdx concentration. A Stern-Volmer plot was created using data points derived from **Equation 2**. PL was the measured photoluminescence at each concentration of Fdx, while PL_0 is the controlled photoluminescence of the nanoparticles when Fdx was not present. The term k_q is the quenching rate constant. τ_0 is the lifetime of the exciton. [Q] is the concentration of the quencher, which is Fdx for this experiment.

$$\frac{PL_0}{PL} = 1 + k_q\tau_0 \cdot [Q] \qquad \textbf{Equation 2}$$

A Langmuir isotherm was used to fit the data and determine a binding constant for Fdx to the nanoparticles, as shown in **Figure 8.B**. The results of this experiment, and the binding

constant derived from this fit, indicate that the ideal concentration of Fdx to work with in these experiments was approximately 100μM.

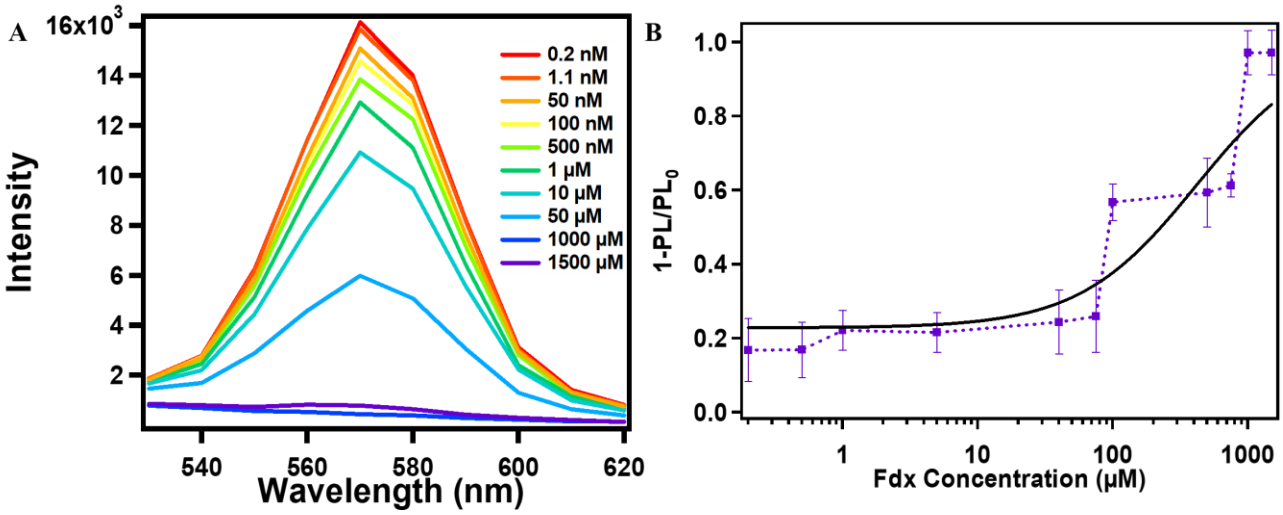

Figure 8: A. Fluorescence measurements of nanoparticles with increasing concentrations of Fdx. **B.** Stern-Volmer plot with a Langmuir isotherm fit.

Lastly, a photoreduction assay was used to characterize the interaction between the nanoparticles and Fdx.. Light-driven ET between the rods and Fdx was monitored by a change in the absorbance spectrum. As shown in **Figure 9.A.,** there are distinctive features present in the absorbance spectrum of both the oxidized and reduced Fdx. The change in absorbance spectrum during the photoreduction assay shows a clear change in the oxidized to reduced state of Fdx. **Figure 9.B** depicts these changing features at 320 nm and 400 nm.

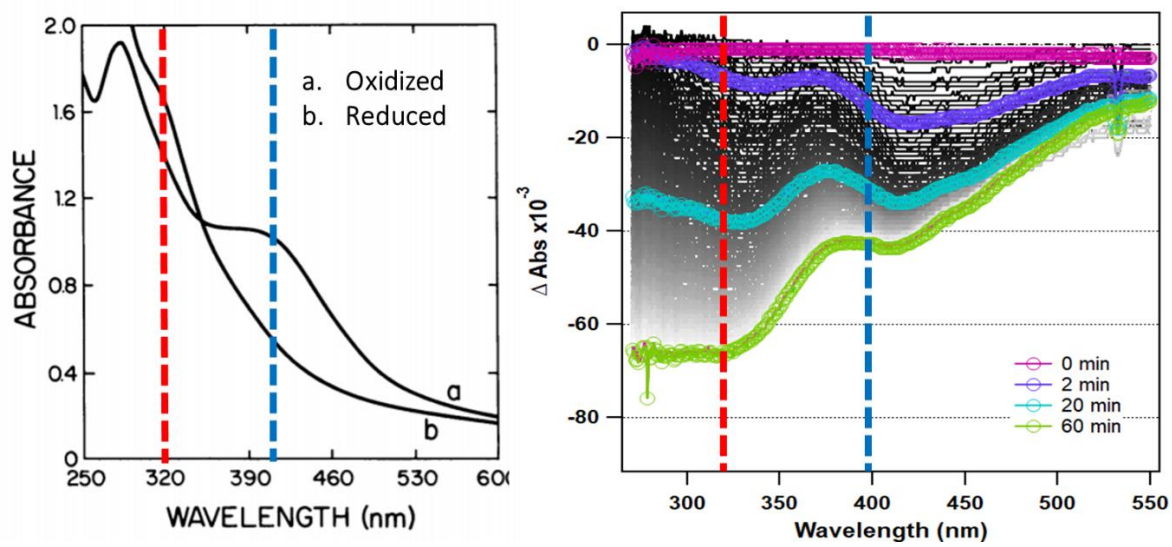

Figure 9: A. Absorbance spectra of oxidized and reduced Fdx from literature.[10]
B. Change in absorbance of photo-reduced Fdx over time.

4.3 Photosensitizer and FMN Interaction

Flavin mononucleotide is considered to be the site of bifurcation.[11] Natively, NADH donates its electron to FMN, which docks onto the bifurcating hydrogenase allowing electron bifurcation to take place. However, in the presence of negatively charged, electron donating photosensitizers, there exists the potential for ET between the nanoparticles and FMN. Similar to studying the interaction between the rods and Fdx, a photoreduction assay was conducted for the rods and FMN. The absorbance spectrum of the oxidized and reduced states of FMN are presented in **Figure 10.A**. The change in absorbance spectrum was monitored as well. **Figure 10.B** shows a distinct negative feature evolving over time, which indicated FMN was being reduced by the nanoparticles.

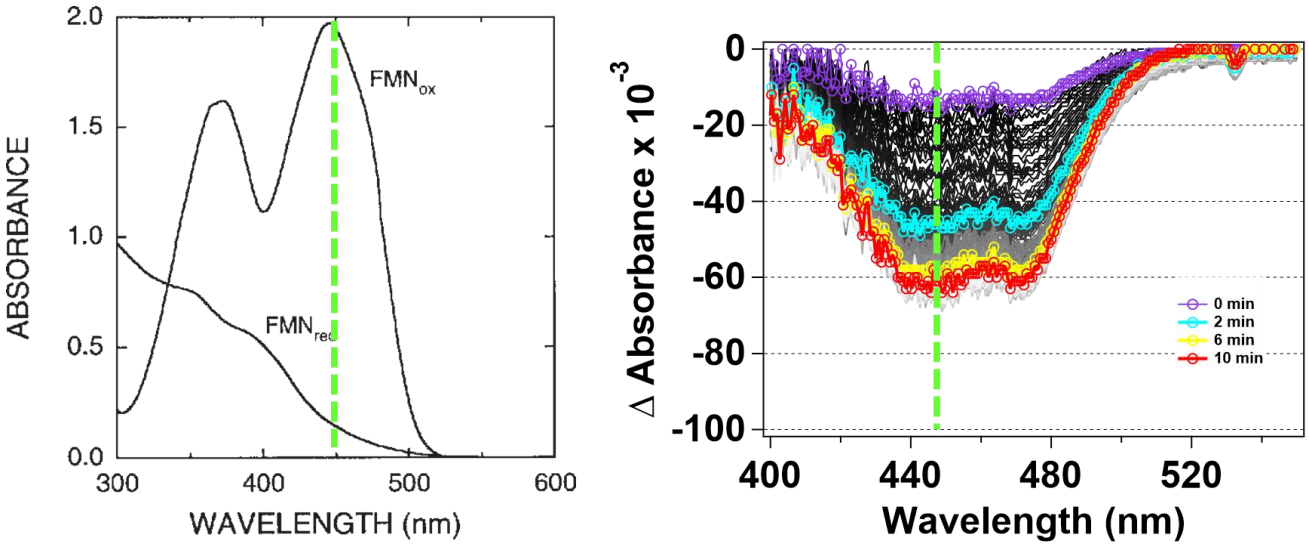

Figure 10: A. Absorbance spectra of oxidized and reduced FMN from literature.[12] **B.** Change in absorbance of photo-reduced FMN over time.

4.4 Photo-driven Hydrogen Production Assays

To characterize the entire system and electron bifurcation, itself, photo-driven hydrogen production assays were conducted. The key to determining whether bifurcation was occurring was by the amount of H_2 generated. It was also previously determined that the rate and amount of hydrogen being produced was a key indicator for bifurcation.[3] Hydrogen production can occur with just the electron transfer from Fdx, but the literature notes that this occurs at a much slower rate. Electron bifurcation should have much greater amounts of H_2 production at a significantly faster rate. To determine the amount of H_2 generated, a pressure sensor mounted into the cap of the reaction vessel was used to monitor the change in pressure. The change in pressure could then be converted to moles of gas using Henry's Law. **Equation 3** shows this relationship. The term "P" stands for the pressure of the gas, "k" is Henry's Law constant, and "C" is the concentration of the gas. "k" is based on the gas, which for H_2 has a value of $7.8 \times 10^{-4} \frac{mol}{kg \times bar}$.[13]

$$P = kC \qquad \textbf{Equation 3}$$

Initial assays, represented by **Figure 11: Assay 1**, showed very minimal hydrogen production. The conditions for these experiments had FMN at a ratio of 500:1 with *Tma*HydABC. There was also a 10:1 ratio between FMN and Fdx, respectively. **Assay 1** had constant illumination of the 532nm diode on the sample. **Figure 11: Assay 2** kept the same conditions except the sample was illuminated in intervals by turning the diode off for 10 minutes at 20-minute intervals, as illustrated by the shaded blocks in **Figure 11**. The rate of hydrogen production did increase significantly when the diode was off compared to when it was on. These results indicated that one of the parts of the system may be short-circuiting electron bifurcation. After reevaluating sample conditions, we determined that the FMN concentration should be decreased to have a 1:1 to ratio with the *Tma*HydABC. Fdx should have also been in excess to have a ratio of 500:1 to *Tma*HydABC. As seen in **Figure 11: Assay 3**, these changes drastically increased the rate of hydrogen production.

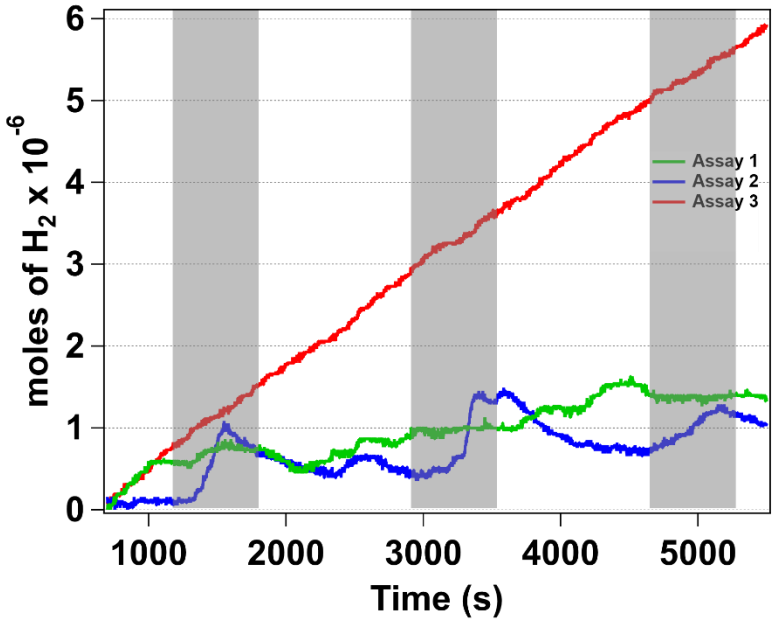

Figure 11: Assay 1. Hydrogen production of bifurcating system measured over time with constant illumination **Assay 2.** Hydrogen production assay with intermittent illumination **Assay 3.** Hydrogen production assay with adjusted conditions, including 1:1 ratio of FMN: *Tma*HydABC

Light-driven ET was still monitored with a change in absorbance. However, as shown in **Figure 3**, the overlap of each components' absorbance spectra made it difficult to follow the individual parts of electron bifurcation. One noticeable element that was observed while monitoring the change in absorbance spectrum, however, was a cyclic feature that appeared at 450nm during trials following **Assay 3**. There was intermittent illumination of the system every 10 minutes. The absorbance feature grew when the light was on and then progressed back to zero when the light was off. **Figure 10.A.** shows a distinct feature at 450nm in the reduced FMN spectrum. It was determined that the flavin was being reduced while the light was on, but when the light was turned off, it transferred its electron to the enzyme. This ET resulted in the absorbance feature to go back to zero, representing the initial, oxidized state of FMN. As there is consistent hydrogen production seen in **Assay 3**, then it can be concluded that FMN is no longer short-circuiting the system and electron bifurcation is occurring. **Figure 12.A.** shows the entire change in absorbance spectrum over 4 minutes for simplification. **Figure 12.B.** shows the cyclic feature that is observed at 450nm over 40 minutes. The shaded gray bars indicate the 10-minute intervals that the laser is turned off.

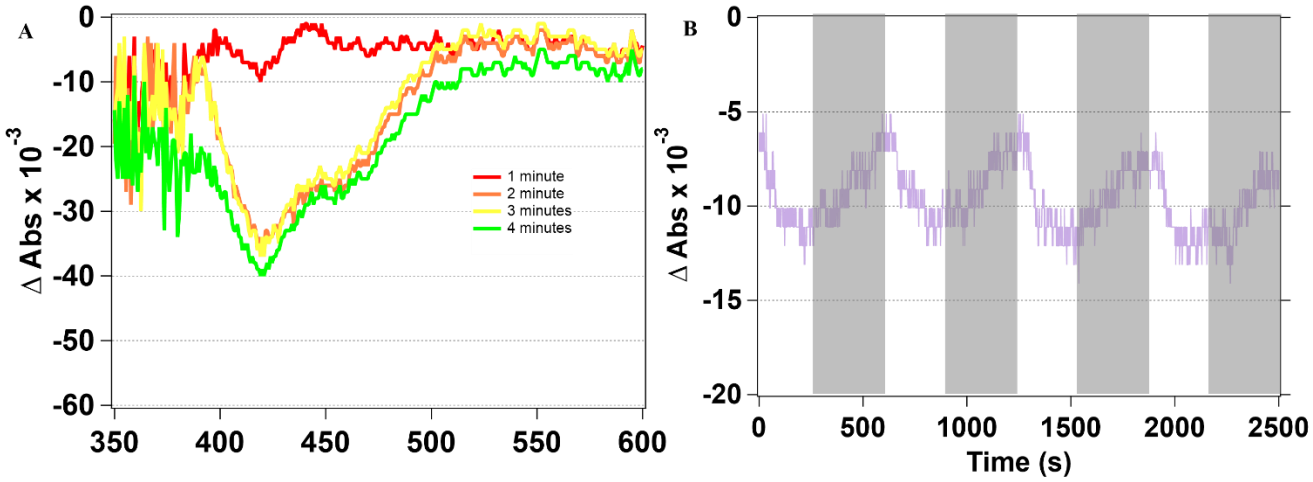

Figure 12: A. Change in absorbance spectrum of entire photocatalytic system with experimental setup for **Assay 3**. **B.** Change in absorbance at 450 nm over 40 minute time period. The grey bars indicate that the photodiode was turned off.

Chapter 5: Conclusions

5.1 Specific Aim 1

The synthesis of the CdSe/CdS nanorods resulted in the successful development of a photosensitizer to be used in the bifurcating photocatalytic system. We were presented with insightful results from the characterization of these the particles, which had the desired physical and electronic properties. Through TEM imaging, we visualized the nanoparticle dimensions and uniformity. The introduction of HPA and a CdS shell both resulted in uniform, rod-like particles. The absorbance spectrum measurements showed no overlap with the cofactors that are used in the photocatalytic system at the excitation wavelength (532 nm). The fluorescence measurements also indicated the light-harvesting abilities of the particles. The greatest evidence, however, came from incorporating the nanorods into a photocatalytic system. The success we saw in the QE experiments, especially the 25% QE with the 532nm diode, solidified our claims for creating the optimal nanoparticles needed for the bifurcating system. We hope to continue to characterize these nanoparticles through nanosecond visible measurements, which would allow us to further study their electronic properties.

5.2 Specific Aim 2

The characterization of the interaction and ET between the nanoparticles and Fdx was successful. With the photoluminescence quenching assay, we saw a decrease in fluorescence with an increase in concentration of Fdx, which indicated an electrostatic interaction occurring between the two species. The photoreduction assays studied key ET pathways between nanoparticles and both Fdx and FMN. Both assays demonstrated efficient ET between the photosensitizer and redox partners. These results also helped establish the optimal conditions that were needed to study the entire system in **Specific Aim 3**. There are further optimization experiments that can be conducted in order to characterize these pathways. Through ultrafast

measurements, we can learn more about the rate of electron transfer between the species in the system.

5.3 Specific Aim 3

The hydrogen production assay was the main source for studying the electron bifurcating mechanism and the *Tma*HydABC system. As forementioned, bifurcation was studied by monitoring H_2 production. Electron bifurcation should have a high rate of H_2 production. Through optimizing the conditions of the system, we saw a significant increase in production. These results have us believe that we did observe electron bifurcation. Further studies to better understand these findings would be the use of time-resolved experiments where we can monitor the system in the infrared and visible light regions. We can study the different catalytic states of *Tma*HydABC and its cofactors to gain insight into the electron bifurcating mechanism.

Chapter 6: Implications of Research

Through incorporating the *Tma*HydABC bifurcating complex into a photocatalytic system, we have not only found a way to study this enzyme but also created a model system to study the electron bifurcation mechanism. As mentioned previously, this mechanism can be replicated as a new source of energy conservation similar to what has been researched for substrate-level phosphorylation and electron-transport linked phosphorylation. The transfer of energy from electrochemical to chemical bonds could be the key to finding new sustainable and renewable sources of energy. For example, the reduction electron bifurcation pathway of the *Tma*HydABC system could potentially be reproduced as a source for renewable fuel storage in the form of H_2. Unfortunately, this cannot be capitalized on until the mechanism itself is understood. That is where the photocatalytic system becomes a significant part of reaching these broader impacts. By first studying the mechanism through a native model, we can understand how nature utilizes electron bifurcation in its evolutionarily optimized form.

References

(1) Komlódi, T.; Tretter, L. Methylene Blue Stimulates Substrate-Level Phosphorylation Catalysed by Succinyl–CoA Ligase in the Citric Acid Cycle. Neuropharmacology 2017, 123, 287–298. https://doi.org/10.1016/j.neuropharm.2017.05.009.

(2) Ashton, T. M.; McKenna, W. G.; Kunz-Schughart, L. A.; Higgins, G. S. Oxidative Phosphorylation as an Emerging Target in Cancer Therapy. Clin Cancer Res 2018, 24 (11), 2482–2490. https://doi.org/10.1158/1078-0432.CCR-17-3070.

(3)Schut, G. J.; Adams, M. W. W. The Iron-Hydrogenase of Thermotoga Maritima Utilizes Ferredoxin and NADH Synergistically: A New Perspective on Anaerobic Hydrogen Production. *Journal of Bacteriology* **2009**, *191* (13), 4451–4457. https://doi.org/10.1128/JB.01582-08.

(4)Peters, J. W.; Beratan, D. N.; Bothner, B.; Dyer, R. B.; Harwood, C. S.; Heiden, Z. M.; Hille, R.; Jones, A. K.; King, P. W.; Lu, Y.; Lubner, C. E.; Minteer, S. D.; Mulder, D. W.; Raugei, S.; Schut, G. J.; Seefeldt, L. C.; Tokmina-Lukaszewska, M.; Zadvornyy, O. A.; Zhang, P.; Adams, M. W. A New Era for Electron Bifurcation. *Current Opinion in Chemical Biology* **2018**, *47*, 32–38. https://doi.org/10.1016/j.cbpa.2018.07.026.

(5) Sanchez, M. L. K.; Konecny, S. E.; Narehood, S. M.; Reijerse, E. J.; Lubitz, W.; Birrell, J. A.; Dyer, R. B. The Laser-Induced Potential Jump: A Method for Rapid Electron Injection into Oxidoreductase Enzymes. J. Phys. Chem. B 2020, 124 (40), 8750–8760. https://doi.org/10.1021/acs.jpcb.0c05718.

(6) Therien, J. B.; Artz, J. H.; Poudel, S.; Hamilton, T. L.; Liu, Z.; Noone, S. M.; Adams, M. W. W.; King, P. W.; Bryant, D. A.; Boyd, E. S.; Peters, J. W. Front. Microbiol. 2017, 8. https://doi.org/10.3389/fmicb.2017.01305.

(7) Manna, L.; Scher, E. C.; Alivisatos, A. P. Synthesis of Soluble and Processable Rod-, Arrow-, Teardrop-, and Tetrapod-Shaped CdSe Nanocrystals. J. Am. Chem. Soc. 2000, 122 (51), 12700–12706. https://doi.org/10.1021/ja003055.

(8) Sanchez, M. L. K.; Wu, C.-H.; Adams, M. W. W.; Dyer, R. B. Optimizing Electron Transfer from CdSe QDs to Hydrogenase for Photocatalytic H_2 Production. Chem. Commun. 2019, 55 (39), 5579–5582. https://doi.org/10.1039/C9CC01150A.

(9) Chica, B.; Wu, C.-H.; Liu, Y.; Adams, M. W. W.; Lian, T.; Dyer, R. B. Balancing Electron Transfer Rate and Driving Force for Efficient Photocatalytic Hydrogen Production in CdSe/CdS Nanorod–[NiFe] Hydrogenase Assemblies. Energy Environ. Sci. 2017, 10 (10), 2245–2255. https://doi.org/10.1039/C7EE01738C.

(10) Aono, S.; Bryant, F. O.; Adams, M. W. A Novel and Remarkably Thermostable Ferredoxin from the Hyperthermophilic Archaebacterium Pyrococcus Furiosus. Journal of Bacteriology 1989, 171 (6), 3433–3439. https://doi.org/10.1128/jb.171.6.3433-3439.1989.

(11) Peters, J. W.; Miller, A.-F.; Jones, A. K.; King, P. W.; Adams, M. W. Electron Bifurcation. *Current Opinion in Chemical Biology* **2016**, *31*, 146–152. https://doi.org/10.1016/j.cbpa.2016.03.007.

(12) Macheroux P. (1999) UV-Visible Spectroscopy as a Tool to Study Flavoproteins. In: Chapman S.K., Reid G.A. (eds) Flavoprotein Protocols. Methods in Molecular Biology, vol 131. Humana Press. https://doi.org/10.1385/1-59259-266-X:1

(13) Hydrogen https://webbook.nist.gov/cgi/cbook.cgi?ID=C1333740&Mask=10 (accessed Nov 13, 2020).